Torsional vibrations of helically buckled drill-strings: experiments and FE modelling

You may also be interested in:

Low dimensional models for stick-slip vibration of drill-strings
M Silveira and M Wiercigroch

Noether symmetry and conserved quantities of the analytical dynamics of a Cosserat thin elastic rod
Wang Peng, Xue Yun and Liu Yu-Lu

On the modelling of Coulomb friction
S J Cull and R W Tucker

The acoustics of the violin: a review
Jim Woodhouse

Torsional vibrations of helically buckled drill-strings: experiments and FE modelling

M Kapitaniak, V V Hamaneh, M Wiercigroch

E-mail: `m.kapitaniak@abdn.ac.uk, vahid.vaziri@abdn.ac.uk, m.wiercigroch@abdn.ac.uk`
Centre for Applied Dynamics Research, School of Engineering, University of Aberdeen, Aberdeen AB24 3UE, UK

Abstract. This paper presents investigations of a complex drill-string vibrations on a novel experimental rig, developed by the Centre for Applied Dynamics Research at the University of Aberdeen. The rig is capable of exhibiting of all major types of drill-string vibrations, including torsional, axial and lateral modes. The importance of this work lies in the fact, that the experimental rig utilizes real industrial drill-bits and rock samples, which after careful identification of Torque On Bit (TOB) speed curves, allows to use an equivalent friction model to accommodate for both frictional and cutting components of the bit-rock interactions. Moreover, the proposed Finite Element model, after a careful calibration, is capable of replicating experimental results, for the prebuckled configuration of the drill-string. This allows us to observe the effect of winding and unwinding of the helical deformation during stick-slip motion.

1. Introduction

The problem of drill-string dynamics has gathered a significant interest in the recent times, due to the importance of identification, understanding and solving problems associated with drilling for oil and gas exploration and extraction. Foremost of those are vibrations of different types, such as torsional, lateral and axial ones, that lead to premature wear and damage of the equipment, that result in fatigue and catastrophic failures. In this paper, we focus our attention on stick-slip phenomenon, which is a self excited vibration mode, happening due to nonlinear characteristics of drill-bit rock interactions, that is of particular interest to the drilling community, due to its negative effect on drilling efficiency [2]. Stick-slip has been analysed in the past using mainly low-dimensional model, based on the torsional pendulum [5, 9, 11, 12, 10] or Finite Element (FE) based models [1, 4, 8].

The structure of this paper is as follows. In Section 2 we describe briefly the experimental setup, which is followed by the description of the FE model. Following, in Section 3 we demonstrate experimental verification of the proposed model and the paper finishes with the conclusions given in Section 4.

2. Experimental rig for investigations of drill-string vibrations

The main objective of the experimental rig developed in the Centre for Applied Dynamics Research, University of Aberdeen, is to provide a comprehensive test bed for investigation of different types of undesired vibrations associated with the industrial drilling for oil and gas exploration and extraction. These include torsional, lateral and axial vibrations. Besides, the
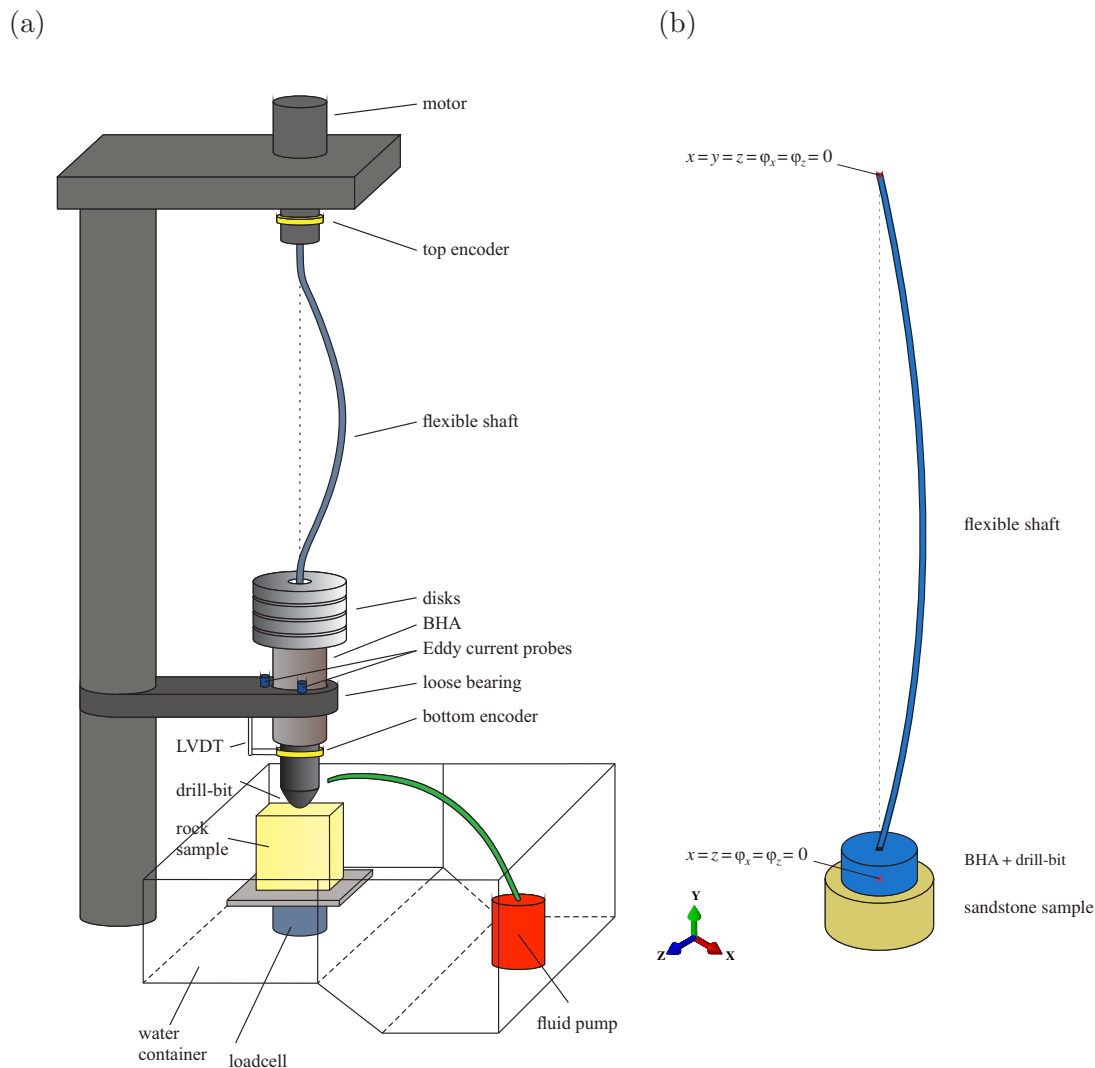
(a)   (b)

Figure 1. (a) Schematic diagram of the experimental rig, where the main components of the system are: sensors (top and bottom encoders, LVDT, eddy current probes and 4-component load-cell), electric motor, flexible shafts, WOB disks, BHA, drill-bit and rock sample. (b) Configuration of the FE model for pre-buckled configuration, showing all the boundary conditions applied at top and bottom nodes.

rig is capable of providing an insight into the interactions between the real industrial drill-bits, used in the setup and various rock samples, which include for example: sandstone, granite and limestone. The schematic of the rig is shown in Fig. 1 (a), where the main components of the setup can be grouped as follows:

- drill-string composed of flexible/rigid shaft, Bottom Hole Assembly (BHA), Weight On Bit (WOB) disks, and the drill-bit,
  - rock samples and cutting fluid circulation system and
  - sensors, instrumentation and Data Acquisition System (DAQ).

The purpose of the current study is to develop a numerical model, which is carefully calibrated based on the experimental setup, described in detail in the following sections. The details about the rig description and the instrumentation used can be found in [7, 6].

As described in [7] , the flexible shaft exhibits different properties depending on direction (e.g. low lateral and high torsional stiffness), and thereby it is required to describe it as an anisotropic material. An orthotropic material has in general different properties along 3 principal axes [3]. Therefore, 9 independent materials constants are required to form elastic matrix $\mathbf{D}$ required to describe the stress-strain relationship, $\sigma = \boldsymbol{D}\varepsilon$. These are three Young's moduli E_1, E_2, E_3, associated with principal axes 1, 2, 3, respectively, three shear moduli G_{12}, G_{13}, G_{23} and three Poisson's ratios ν_{12}, ν_{13}, ν_{23} for planes 1-2, 1-3, 2-3, respectively. The relation between the strain and the stress, $\varepsilon = \boldsymbol{D}^{-1}\sigma$, can be expressed in matrix form as:

$$
\begin{pmatrix} \varepsilon_{11} \\ \varepsilon_{22} \\ \varepsilon_{33} \\ \gamma_{12} \\ \gamma_{13} \\ \gamma_{23} \end{pmatrix} = \begin{pmatrix} \frac{1}{E_1} & \frac{-\nu_{21}}{E_2} & \frac{-\nu_{31}}{E_3} & 0 & 0 & 0 \\ \frac{-\nu_{12}}{E_1} & \frac{1}{E_2} & \frac{-\nu_{32}}{E_3} & 0 & 0 & 0 \\ \frac{-\nu_{13}}{E_1} & \frac{-\nu_{23}}{E_2} & \frac{1}{E_3} & 0 & 0 & 0 \\ 0 & 0 & 0 & \frac{1}{G_{12}} & 0 & 0 \\ 0 & 0 & 0 & 0 & \frac{1}{G_{13}} & 0 \\ 0 & 0 & 0 & 0 & 0 & \frac{1}{G_{23}} \end{pmatrix} \begin{pmatrix} \sigma_{11} \\ \sigma_{22} \\ \sigma_{33} \\ \sigma_{12} \\ \sigma_{13} \\ \sigma_{23} \end{pmatrix}. \tag{1}
$$

For details of calibration of the torsional properties of the FE model of the flexible shaft, please refer to [7]. In order to evaluate the bending characteristics of the flexible shaft, which are of high importance for modelling of the prebuckled configuration described in the previous section, we perform a series of simple experiments. Therefore, the length of the flexible shaft is limited to 20 cm, by clamping the flexible shaft at the appropriate length, as shown in Fig. 2(a).

As a result, we have a system that is equivalent to cantilever beam, with fixed-free boundary conditions. As can be seen in Fig. 2(a), the flexible shaft on the right hand side has an end fitting (of mass 0.091 kg), which coupled with the weight of the flexible shaft section, results in an end deflection. This state of the flexible shaft is considered as an initial reference configuration. Furthermore, to test bending mechanical properties, we attach to the end of the flexible shaft a number of disks of equal mass (100 g), and observe the resultant end deflection. This is shown in Fig. 2(b)-(c), which correspond to loading with 1-8 disks, respectively. Moreover, the cable behaves in a consistent way, regardless the direction of bending, as can be seen in Fig. 2(d), which presents experimental results of end deflection for both transversal directions, as a function of number of disks attached at flexible shafts end. Clearly, the symmetry in transversal direction is observed. The measurements of experimental end deflection, have been conducted using image recognition technique, which shows that both transversal deflections are consistent, as shown in Fig. 2(d).

One of the critical steps in the modelling of drill-string dynamics is the mathematical description of the bit-rock interactions. Quantitatively, these interactions are represented in terms of Torque On Bit (TOB) versus bit velocity curves, which need to be appropriately modelled. For this purpose, we will follow the approach described [7], where the main idea behind it, is to use suitable effective friction coefficient (slip-rate dependent) that captures the main phenomena observed in our drilling tests, namely, cutting and friction between the drill-bit and the rock sample. According to drilling tests conducted in [7] a presence of the Stribeck effect [13] can be observed, therefore the friction model to be used for the mathematical description of the bit-rock interaction is

$$
\mu(r, \omega_b) = \mu_k + (\mu_s - \mu_k)\, e^{-d_c r \omega_b} + \mu_{str} r \omega_b, \tag{2}
$$

where μ_k, μ_s, μ_{str} and d_c represent the kinetic, static, Stribeck friction coefficient and the decay rate respectively. Based on that, as described in [7], the resultant TOB function is given by
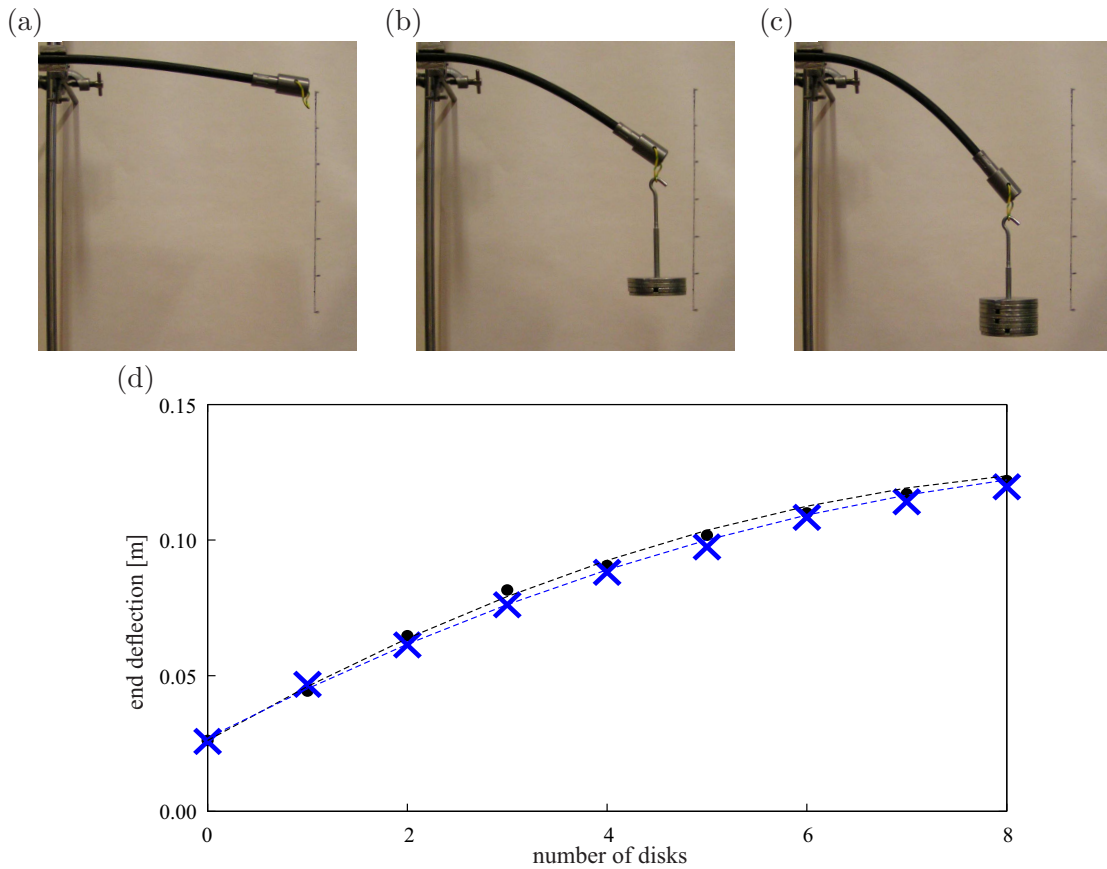
(a)   (b)   (c)

(d)

Figure 2. Experiments to determine mechanical characteristics of the flexible shaft. Examples of static bending of a flexible shaft (a)-(c) subjected to different loading conditions and (d) corresponding end deflections of a flexible shaft, subjected to different loading (number of disks) for both transversal directions (denoted with dots and crosses).

$$
T_{b,sl}(\omega_b) = \begin{cases} \dfrac{2}{3}\lambda_s W_b, & \omega_b = 0, \\[2ex] \dfrac{2}{3}\lambda_k W_b + \dfrac{2W_b(\lambda_s - \lambda_k)}{\lambda_d^3 \omega_b^3}\left(2 - e^{-\lambda_d \omega_b}\left(\lambda_d^2\omega_b^2 + 2\lambda_d\omega_b + 2\right)\right), & \omega_b > 0, \\[2ex] +\dfrac{1}{2}W_b\lambda_{str}\omega_b \end{cases} \tag{3}
$$

where $\lambda_s = \mu_s R$, $\lambda_k = \mu_k R$ and $\lambda_d = d_c R$, $\lambda_{str} = \mu_{str} R^2$, ω_b and R represent angular velocity and radius of the drill-bit. Based on the experimental results, a curve fitting of the experimental TOB (See Fig. 3 (a)) to the Eq. (3) was performed, which allows to obtain necessary parameters for equivalent friction coefficients (see Fig. 3 (b)) corresponding to torque curves for each WOB case. All the necessary parameters to construct experimental torque curves are given in Table 1.

Table 1. Parameters of the equivalent friction coefficients describing bit-rock interactions.

W_b [kN]	λ_s	λ_k	λ_d	λ_{str}
2.19	0.0059	0.0051	0.3091	1.4890E-05
2.06	0.0068	0.0051	0.3678	5.9844E-06
1.88	0.0063	0.0044	0.1219	1.7256E-05
1.57	0.0058	0.0044	0.1770	2.3248E-05
1.43	0.0063	0.0043	0.1085	2.0700E-05
1.22	0.0059	0.0046	0.1298	1.8227E-05
1.10	0.0058	0.0036	0.0695	3.4923E-05
0.94	0.0000	0.0045	0.0000	0.0000E+00
0.85	0.0000	0.0044	0.0000	0.0000E+00
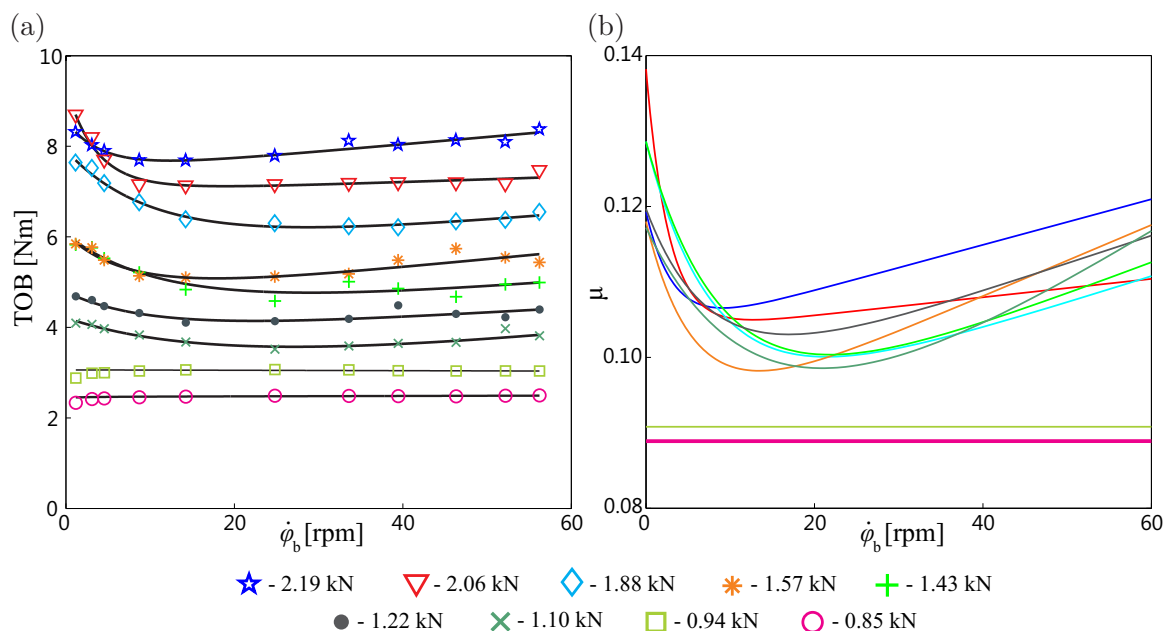
Figure 3. (a) Experimental identification of TOB curves for different WOB conditions (b) Corresponding equivalent friction coefficients as a function of bit velocity.

3. Experimental verification

Firstly we consider a response of stick-slip oscillations, for initial pre-buckling of $d_{pb} = 0.0381$ m (axial downward displacement) and WOB value of $W_b = 1.45$ kN, whose time history and phase portrait are shown in Fig. 4 (a). As can be seen, one observe stick-slip oscillations of constant amplitude, which are the result of small oscillations of the top speed and induced buckling of the flexible shaft. In order to replicate this kind of response in the FE model, we fit the top excitation (black curves in Figs. 4 (a)-(b)) using Fourier series:

$$\dot{\varphi}_t = a_0 + \sum_{n=1}^{6} a_n \cos(n\omega_p t) + \sum_{n=1}^{6} b_n \sin(n\omega_p t), \tag{4}$$

where $a_0 = 3.421\,\text{rad/s}$, $a_1 = 0.0001082\,\text{rad/s}$, $b_1 = 0.001583\,\text{rad/s}$, $a_2 = 0.0006394\,\text{rad/s}$, $b_2 = -0.001014\,\text{rad/s}$, $a_3 = 0.0001515\,\text{rad/s}$, $b_3 = -0.0009761\,\text{rad/s}$, $a_4 = -0.0006725\,\text{rad/s}$, $b_4 = 0.001115\,\text{rad/s}$, $a_5 = -0.01963\,\text{rad/s}$, $b_5 = -0.01733\,\text{rad/s}$, $a_6 = 0.0001247\,\text{rad/s}$,
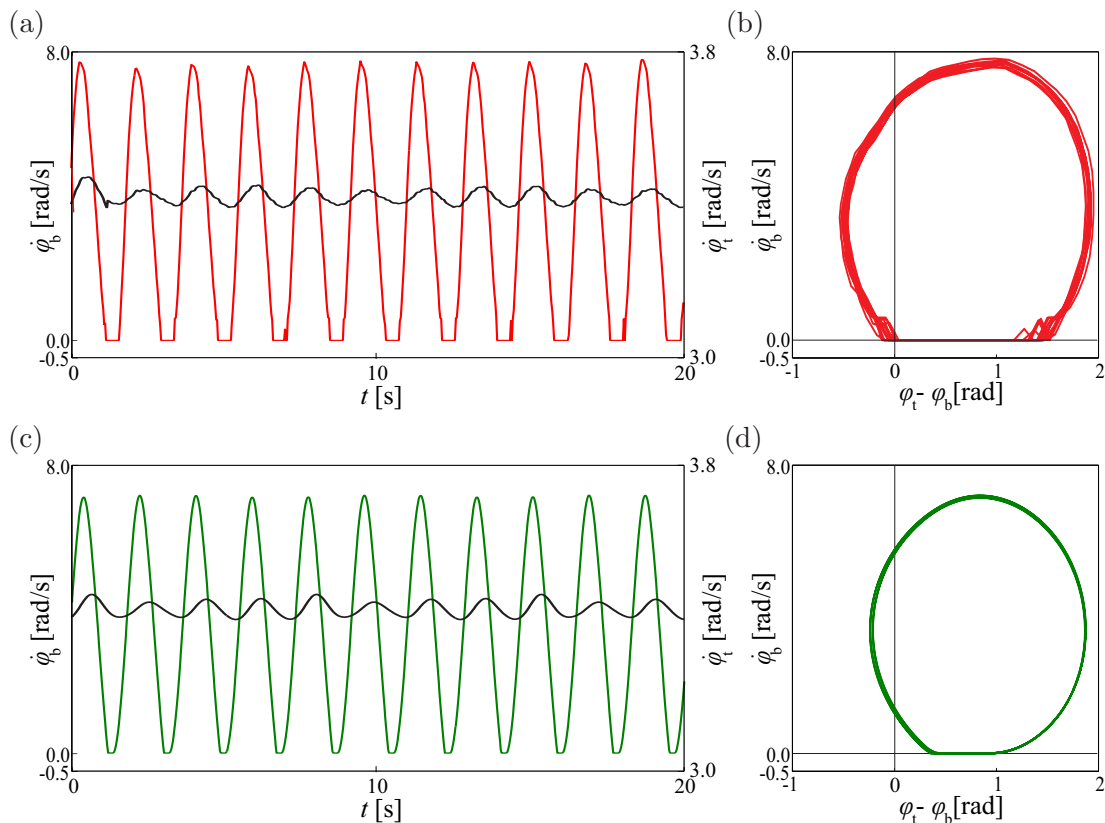
Figure 4. An example of stick-slip oscillations occurring in the experimental rig for pre-buckled configuration (d_{pb} = 0.0381 m) and W_b=1.45 kN (time history (a), phase portrait (b)) and corresponding response for FE model (time history (c), phase portrait (d))

$b_6 = -0.003006$ rad/s, $\omega_p = 0.6836$ rad/s. As a next step we choose the appropriate parameters for TOB model (see Eq. (3) and Table 1), that correspond to the measured WOB of $W_b = 1.45$ kN. As can be seen in Fig. 1 (b), we apply initial axial displacement $d_{pb} = 0.381$ m at the top of the flexible shaft, in order to induce buckling of the flexible shaft, which corresponds directly to the experimental conditions. For this particular case we assign corresponding mass and inertia to the reduced drill-bit and BHA (see Fig. 1 (b)): $m_{\mathrm{BHA}} = 148.579$ kg and $J_{\mathrm{BHA}} = 0.8416$ kg m^2, taking into account effect of gravity ($g = 9.81$ m/s^2). The following parameters of the flexible shaft: $E_1 = E_2 = 3.64\,\mathrm{GPa}$, $E_3 = 1.50\,\mathrm{GPa}$, $G_{12} = 0.02\,\mathrm{GPa}$, $G_{13} = G_{23} = 18.16\,\mathrm{GPa}$, $\nu_{12} = \nu_{13} = \nu_{23} = 0.30$ and $\alpha = 7.50$ have been used. As can be seen in Fig. 1(b), the FE model of the experimental setup consists of two cylinders, one representing the drill-bit and the other the rock sample, and the flexible shaft set in the prebuckled configuration, which allows us to observe helical buckling condition.

As can be seen in Fig. 4(b), we are able to obtain a good qualitative and quantitative agreement between experiment and our FE model. Note, that there are small differences, as the model predicts slightly smaller amplitude of stick-slip vibrations, while keeping the same period. At the same time, when comparing the phase portraits for both cases, we observe that the sticking interval is also slightly smaller than the one observed in experiment, which might be caused by the simplification of cutting process using an equivalent friction approach.

In Fig. 6 (a)-(b) and Fig. 5 (a)-(b) we present the comparison of the shapes of the flexible shaft, during different stages of observed stick-slip oscillations, for front and top view respectively. Note, that the scale of pictures taken during experiment and from the FE model is not the
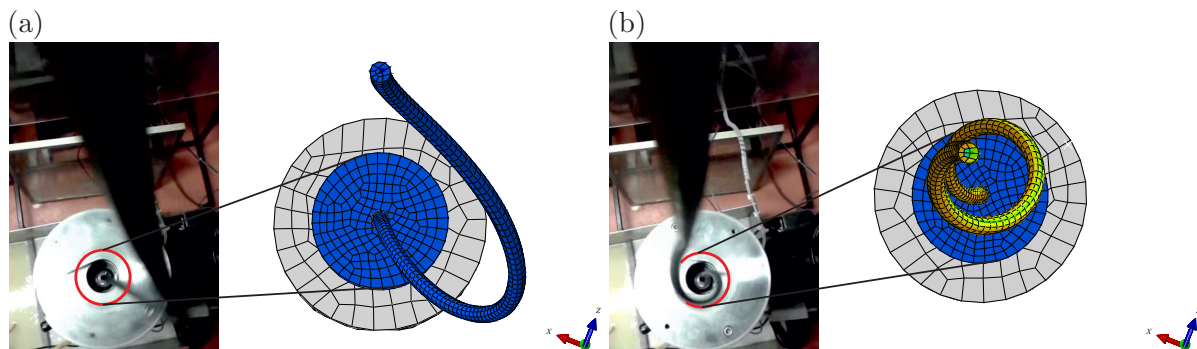
Figure 5. Comparison of shape of the flexible shaft during stick-slip oscillations for experiment and FE model (top view), whose time history is shown in Fig. 4
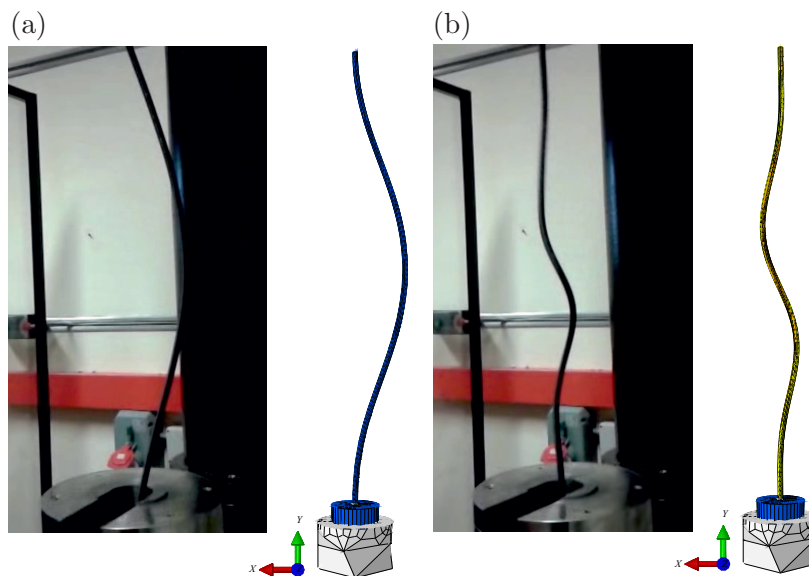

Figure 6. Comparison of shape of the flexible shaft during stick-slip oscillations for experiment and FE model (front view), whose time history is shown in Fig. 4

same. The size of the red circle, as introduced in photos from experiment(Fig. 5 (a)-(b)) corresponds directly to the size of blue cylinder representing the drill-bit in the FE model. As the drill-bit is in motion, the flexible shaft takes the shape of the initial configuration as shown in Fig. 6 (a) and Fig. 5 (a), but once the drill-bit stops we observe an abrupt change, as the flexible shaft takes the shape of a helix (see Fig. 6 and Fig. 5 (b)). As during the sticking phase, the top continues to rotate, we observe an increasing torsional deformation of the flexible shaft, until the moment that enough energy to overcome the static torque is stored in the shaft. Once that happens we observe unwinding of the helix formed. Finally the flexible shaft takes the shape of Fig. 6 (a) and Fig. 5 (a) and the whole cycle is repeated. Clearly, from Figs. 5 and 6 it is visible that we are able to obtain a good agreement between the experimental time histories and the FE predictions.

4. Conclusions and future work

In this paper, an experimental verification of the developed FE model of the drilling rig introduced in [7, 6] is carried out. In general a flexible shaft used to replicate the drill-string in the experimental conditions can be driven in two configurations: straight and buckled. In this work we concentrated our attention on latter case, to shed some light on the complexity of the helical buckling phenomenon. Thereby, based on a careful identification of all the experimental parameters, one is able to adjust the FE model to replicate appropriately the results recorded on the experimental rig. It is demonstrated that both the qualitative and quantitative agreements between experiments and the FE model are achievable. The developed model is capable of predicting accurately the shape of the flexible shaft during different phases of stick-slip phenomena, as shown in Figs. 5 and 6. In view of positive verification of the developed FE model, we can conclude that the model applicability has been demonstrated and further analysis of the model will be conducted, with a particular attention to parameters controlling onset of stick-slip phenomenon.

Acknowledgements

References

[1] H. Al-Naser and Y.A. Khulief. Finite element dynamic analysis of drillstrings. *Finite Elements in Analysis and Design*, 41(13):1270–1288, 2005.

[2] A.M Chevallier, N.P Politis, M.L Payne, and P.D. Spanos. Oil and gas well drilling: A vibrations perspective. *Shock and Vibration Digest*, 35(2):85–103, 2003.

[3] Dassault Systemes Simulia Corp. *ABAQUS Theory Manual and Analysis User's Manual (Version 6.12)*, 2010.

[4] H. Hakimi and S. Moradi. Drillstring vibration analysis using differential quadrature method. *Journal of Petroleum Science and Engineering*, 70(3-4):235–242, 2010.

[5] J. D. Jansen and L. van den Steen. Active damping of self-excited torsional vibrations in oil well drillstrings. *Journal of Sound and Vibration*, 179(4):647–668, 1995.

[6] M. Kapitaniak. *Nonlinear Dynamics of Drill-strings*. PhD thesis, University of Aberdeen, 2015.

[7] M. Kapitaniak, V. Vaziri Hamaneh, J. Páez Chávez, and M. Wiercigroch. Unveiling Complexity of Drill-String Vibrations: Experiments and Modelling. *International Journal of Mechanical Sciences*, 101-102:324–337, 2015.

[8] Al-Naser H. Khulief, Y.A. Finite element dynamic analysis of drillstrings. *Finite Elements in Analysis and Design*, 41(13):1270–1288, 2005.

[9] R. I.. Leine, D. H. van Campen, A. de Kraker, and L. van den Steen. Stick-Slip vibrations induced by alternate friction models. *Nonlinear Dynamics*, 16(1):41–54, 1998.

[10] C. Liao, B. Balachandran, M. Karkoub, and Y.L. Abdel-Magid. Drill-string dynamics: Reduced-order models and experimental studies. *Journal of Vibration and Acoustics*, 133((4)), 2011.

[11] E. M. Navarro-López. An alternative characterization of bit-sticking phenomena in a multi-degree-of-freedom controlled drillstring. *Nonlinear Anal. Real World Appl.*, 10(5):3162–3174, 2009.

[12] E. M. Navarro-López and D. Cortés. Avoiding harmful oscillations in a drillstring through dynamical analysis. *Journal of Sound and Vibration*, 307:152–171, 2007.

[13] J. Wojewoda, A. Stefanski, M. Wiercigroch, and T. Kapitaniak. Hysteretic effects of dry friction: modelling and experimental studies. *Philosophical Transactions of the Royal Society A*, 366:747–765, 2008.